Double and single peaks in nuclear magnetic resonance spectra of natural and ^{29}Si-enriched single-crystal silicon

Anne S. Verhulst,* Denis Maryenko,† and Yoshihisa Yamamoto‡
Quantum Entanglement Project, ICORP, JST, E.L. Ginzton Laboratory, Stanford University, Stanford, California 94305-4088, USA

Kohei M. Itoh
Department of Applied Physics and Physico-Informatics, Keio University and CREST-JST, Yokohama 223-8522, Japan
(Received 21 November 2002; revised manuscript received 20 February 2003; published 7 August 2003)

We report the nuclear magnetic resonance (NMR) spectra of phosphorus-doped single-crystal silicon, enriched to 97% ^{29}Si, which display double as well as single peaks as the sample is rotated with respect to the static magnetic field. It is shown that the shape and the width of the NMR lines are predominantly due to nuclear dipolar interactions. We provide a theoretical model to determine the strength of the weaker scalar coupling between neighboring ^{29}Si nuclei. For naturally abundant single-crystal silicon (4.7% ^{29}Si), the anisotropic dipolar interaction is visible as well in the NMR spectra. We have observed small side peaks for particular orientations of the crystal axes and we show that the intensity of the side peaks contains information on the distribution of ^{29}Si atoms in the ^{28}Si matrix.

DOI: 10.1103/PhysRevB.68.054105 PACS number(s): 61.66.−f, 82.56.−b, 03.67.Lx, 76.60.−k

I. INTRODUCTION

Intensive research has been performed on single-crystal silicon, which is the workhorse of the microelectronics industry today, in order to fully understand the material and control its quality. Recently published quantum computation proposals[1,2] are also based on silicon and rely on the existing expertise. Since the gate operation of these proposed quantum computers depends on the interaction between nuclear magnetic moments, detailed information on this interaction is very important. Reference 2, for example, proposes the direct use of the state of the ^{29}Si nuclear spin as a qubit. It is therefore highly relevant to obtain information on the line shape and width of the NMR resonance lines, which is related to the coherence time of a nuclear spin system, and on the scalar coupling between ^{29}Si nuclei, which contributes to the gate operation time. Researchers have independently made efforts to isotopically purify silicon and produce high quality single crystals.[3] Naturally abundant silicon contains 92.2% ^{28}Si (nuclear spin 0), 4.7% ^{29}Si (nuclear spin $\frac{1}{2}$), and 3.1% ^{30}Si (nuclear spin 0). Single-crystal wafers of pure ^{28}Si are already commercially available[4] and research is ongoing towards the production of isotopically pure ^{29}Si and ^{30}Si single crystals. Silicon samples with various concentrations of the ^{29}Si isotope are very interesting to study with NMR spectroscopy, since the effect of the isotopic concentration on phenomena such as optical pumping[5,6] and spin diffusion can be investigated.

We report on the NMR spectra of ^{29}Si-enriched silicon, which reveal a strong dependence on the orientation of the crystal axes versus magnetic field. We start the theoretical modeling of the data with a qualitative analysis of all mechanisms that could modify the silicon NMR spectrum and show that dipole-dipole coupling produces the strongest nuclear interaction. Using a model based on this interaction, we provide a quantitative analysis of the experimental data. Then, we expand the model to include scalar coupling and explain how more quantitative information on the strength of this interaction could be obtained. We have performed similar experiments with naturally abundant silicon samples, for which we have observed small side peaks adjacent to the main resonance peak. We show that the ratio of the area under the side peaks to the area under the main peak gives information on the distribution of the ^{29}Si atoms in a ^{28}Si matrix.

II. EXPERIMENTAL SETUP

Single-crystal silicon has a diamond structure (see unit cell and main axes in Fig. 1). The ^{29}Si isotopically enriched sample is a single-crystal cylinder, with an approximate diameter of 8 mm and a height of 4.5 mm. The growth axis is [100], but the sample has been cut off-axis and there is about 5° uncertainty in the exact orientation of the crystal axes. The isotopic concentration of this sample is 2.4% ^{28}Si, 96.9% ^{29}Si, and 0.7% ^{30}Si, and the phosphorus doping level is $1-2\times10^{15}$ cm^{-3}. The latter determines the spin-lattice relaxation time T_1, which has been measured to be 138 $\pm$10 min, in agreement with theoretical predictions.[7]

The naturally abundant sample consists of a stack of eight 8×8-mm^2 pieces of silicon wafer (single crystal), producing a total sample height of 4 mm. The wafer orientation is [100] and the wafer pieces have been cut parallel to $\langle110\rangle$ directions. The isotopic concentration is 92.2% ^{28}Si, 4.7% ^{29}Si, and 3.1% ^{30}Si, and the phosphorus doping level $1-4\times10^{15}$ cm^{-3}.

The samples are inserted in the holder of a homebuilt probe and can be rotated along the central axis of the RF coil, with a precision of 0.5°. Accurate initial positioning of the samples is hard, especially for the ^{29}Si-enriched sample, due to the miscut of the crystal. Therefore, the NMR spectra we show correspond to the specified orientations within 10° error.

The NMR spectra are taken at room temperature with a commercial spectrometer (Tecmag) in a 7-T magnet (Oxford

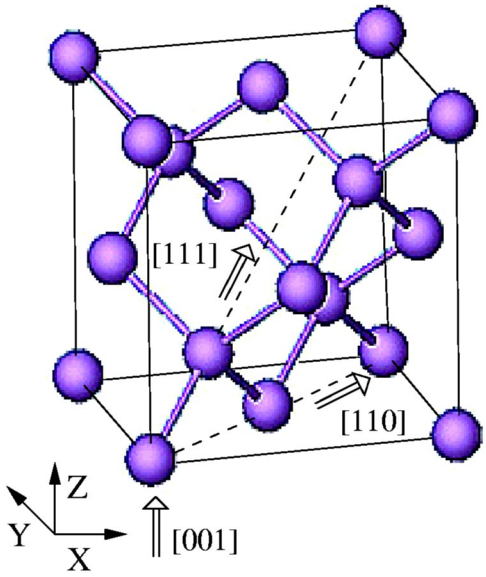

FIG. 1. Unit cell of the diamond structure. As can be seen, the bonds lie along ⟨111⟩ directions.

Instruments). This magnetic field corresponds to a Larmor frequency of $f_{Si}=59.5744$ MHz. The pulse sequence consists of a $\pi/2$ pulse (30 μsec), followed by a 5-μsec dead time and the observation of the free induction decay. The presented spectra are the real part of the Fourier transform of the free induction decay, starting 30 μsec after the beginning of the data acquisition. Time intervals between two successive experiments range from 30 min to 3 h since T_1 is very long for all samples (more than 2 h).

III. EXPERIMENTAL RESULTS FOR ^{29}Si-ENRICHED SILICON

The NMR spectra for the ^{29}Si-enriched sample are shown in Fig. 2 for 21 orientations of the sample with respect to the magnetic field. The crystal is first oriented with the [001] axis parallel to the magnetic field B_0 and then rotated along the [110] axis, such that B_0 becomes parallel to [001], $[1\bar{1}1]$, $[1\bar{1}0]$, $[1\bar{1}\bar{1}]$, and $[00\bar{1}]$, consecutively. The experimental data show a strong dependence on the orientation of the magnetic field with respect to the crystal structure. The resonance lines are most narrow for ⟨100⟩ orientations (~800 Hz), become very broad for ⟨110⟩ orientations (~2000 Hz), and a line splitting appears for ⟨111⟩ orientations (maximum observed line splitting of 1250 Hz). The spectra have been normalized such that the total area underneath each spectrum is the same, to compensate for the varying initial polarizations of consecutive experiments (we have observed area fluctuations of ±5% over the whole range of crystal orientations when the initial state of the spin system for each experiment is identical).

IV. THEORETICAL MODEL

In a diamond lattice, every silicon atom is tetrahedrally surrounded by four nearest neighbors (see Fig. 1). The ori-

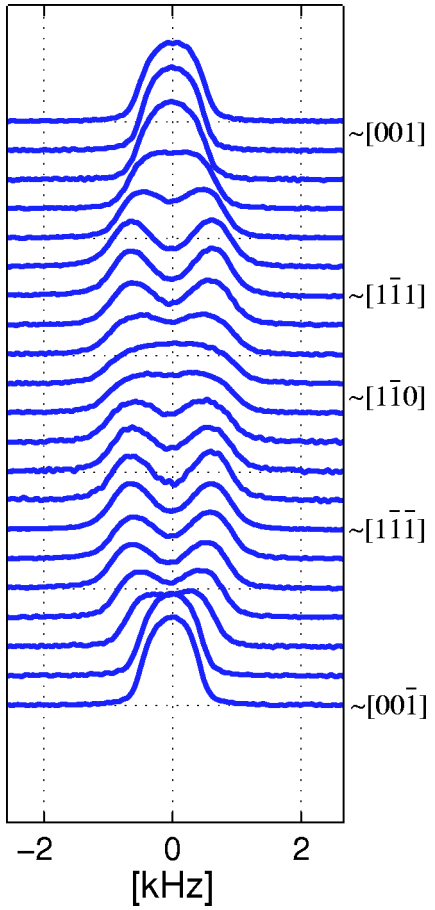

FIG. 2. NMR spectra of a ^{29}Si isotopically enriched single-crystal silicon sample. The horizontal axis is offset by 59.5744 MHz; the vertical axis is arbitrary. The sample is rotated by ~10° along the [110] axis between subsequent experiments. The width of the resonance line for the ⟨100⟩, ⟨110⟩, and ⟨111⟩ orientations is ~800 Hz, ~2000 Hz, and ~800 Hz, respectively. A maximum line splitting of 1250 Hz is observed in ⟨111⟩ orientations.

entation of the bonds belongs to the set of ⟨111⟩ directions. Assuming no crystal strain and negligible bond changes due to isotopic variation,[8] all nuclear sites are magnetically equivalent since silicon has T_d point-group symmetry.[9] Therefore, the effect of chemical shift anisotropy in NMR spectra can be neglected. As mentioned above, only one isotope, ^{29}Si, can be observed with NMR spectroscopy. Since ^{29}Si has nuclear spin $I=\frac{1}{2}$, no nuclear quadrupolar interactions are present and only direct and indirect nuclear dipolar interactions determine the resonance spectra of single-crystal silicon.

There are two types of indirect dipolar interactions: the Ruderman-Kittel-Kasuya-Yosida (RKKY) interaction,[10] which is a long-range interaction, and the scalar coupling or *J*-coupling, which is a short-range interaction. The RKKY interaction is normally observed in NMR spectra of heavy metals and the strength of the interaction is proportional to the square of the density of the conduction electrons. All of the silicon samples in the present experiments are *n*-type with phosphorus doping levels $\leqslant 4\times10^{15}$ cm^{-3}. Therefore, the RKKY-type interactions will cause changes in the line-

width of the resonance peaks which are far below 1 Hz. Considering the data in Fig. 2, this type of indirect nuclear interaction can be neglected. Theoretical predictions of the other type, scalar coupling, have been made for the lightest atoms,[11] up to ^{23}Na, but the calculations are increasingly hard if more electron shells are involved. Experimental research reports scalar coupling constants of 23–186 Hz for ^{29}Si-^{29}Si single bonds.[12] Such a coupling strength can at most account for a small part of the spectral features we observe in Fig. 2. Direct magnetic dipolar interactions between two neighboring ^{29}Si nuclear spins in single-crystal silicon produce couplings of up to 1000 Hz and from the observed linewidth in Fig. 2, it is clear that this is the right order of magnitude for explaining our data.

Finally, since T_1 for the silicon samples is very long (several hours) and in agreement with theoretical predictions based on the doping type and concentration,[7] nuclear interactions with magnetic impurities should be very weak and will also be neglected in our discussion. The interaction with the phosphorus nuclei themselves (nuclear spin $\frac{1}{2}$, 100% abundant) is also negligible, because of density considerations (the atomic density of single-crystal silicon is 5×10^{22} cm^{-3}). The structure of our system is therefore a lattice of spin-$\frac{1}{2}$ nuclei, coupled via magnetic dipolar interactions. The effect of the scalar coupling is discussed later.

Previous experiments have observed line splittings in NMR spectra of particular samples in which the dominant nuclear interaction is a dipolar interaction.[13,14] The original experiment[13] was performed with a sample containing fairly isolated pairs of ^{1}H nuclei. When the magnetic field B_0 was parallel to the axis connecting ^{1}H pairs, a symmetric double peak appeared in the NMR spectrum.[13] This phenomenon, called a Pake's doublet, has been observed more recently for a ^{13}C-enriched single-crystal diamond sample.[14] In this case, the nuclei are no longer isolated, but anisotropy of the dipolar interaction creates semi-isolated pairs of ^{13}C nuclear spins. Since silicon has a diamond structure as well and the dominant interaction is dipolar coupling, the discussion for the ^{29}Si-enriched sample is analogous to the ^{13}C case.

The truncated Hamiltonian $H_{\rm dd}$ of a system of identical magnetic dipoles $\boldsymbol{\mu}_{\rm Si}=\gamma_{\rm Si}\hbar\boldsymbol{I}_{\rm Si}$ is given by[16]

$$H_{\rm dd}=\frac{\mu_0}{4\pi}\gamma_{\rm Si}^2\hbar^2\sum_{i<j}\frac{(3I_i^zI_j^z-\boldsymbol{I}_i\boldsymbol{I}_j)}{2r_{ij}^3}(1-3\cos^2\theta_{ij}), \quad (1)$$

with $\gamma_{\rm Si}$ the gyromagnetic ratio of ^{29}Si, $\boldsymbol{I}_i$ the nuclear angular momentum vector of nucleus i, r_{ij} the distance between the positions of two nuclei i and j, and θ_{ij} the angle between the magnetic field B_0 and the vector $\boldsymbol{r}_{ij}$. The last factor in Eq. (1) shows that the dipole-dipole interaction between two nuclei is dependent on the arrangement of the atoms with respect to the magnetic field. The strongest interaction occurs if $\boldsymbol{r}_{ij}$ is parallel to B_0 and the interaction completely vanishes if $\boldsymbol{r}_{ij}$ is at the magic angle $\theta_{ij}=54.74°$. The strength of the dipolar interaction is directly reflected in the width of the resonance lines in the NMR spectra. We consider three crystal orientations:

(i) B_0 parallel to [100]: all four nearest neighbors are at the magic angle with respect to B_0 and only second-nearest-neighbor interactions and higher contribute to the linewidth. Therefore, a relatively narrow resonance line is expected.

(ii) B_0 parallel to [110]: two nearest neighbors are at 35.3° with respect to B_0 and two are at 90°. The interaction between a given nucleus and any one of its nearest neighbors therefore causes a line splitting of[13]

$$\Delta f=\frac{1}{2\pi}\frac{\mu_0}{4\pi}\frac{\gamma_{\rm Si}^2\hbar}{r_{ij}^3}\frac{3}{2}=550\ \text{Hz} \quad (2)$$

and depending on the exact spin configuration of the four nearest neighbors, several NMR peaks will appear with a maximum splitting of 4×550 Hz$=2200$ Hz. There are contributions from the second-nearest neighbors as well and overall, a relatively broad resonance line is expected.

(iii) B_0 parallel to [111]: one bond is parallel to B_0 and this produces the strongest possible interaction; the other three are at 70.5° and the interaction with each one of them is weaker by a factor of 3. If only the bond parallel to B_0 is considered, a Pake's doublet[13] would be observed with line splitting

$$\Delta f=\frac{1}{2\pi}\frac{\mu_0}{4\pi}\frac{\gamma_{\rm Si}^2\hbar}{r_{ij}^3}3=1100\ \text{Hz}. \quad (3)$$

Including contributions from the other nuclei, two relatively broad resonance lines with the above splitting are expected.

V. RESULTS AND DISCUSSION

The data in Fig. 2 correspond very well to the intuitive picture described above and are also in good agreement with the spectra obtained for ^{13}C-enriched diamond,[14] taking into account a scaling factor of 5.6 [see the dependence on gyromagnetic ratio and lattice constant in Eqs. (1)–(3)]. The line splitting and linewidth for the resonance line in the $\langle111\rangle$ orientation (see Fig. 2, caption) have been determined by fitting the NMR spectrum with two Gaussian-shaped curves. We have also performed an experiment in which the initial orientation of the sample is [110], with rotation along the [001] direction. In this case, the NMR spectra change from a single broad peak to a single narrow peak and back to a single broad peak, without displaying the double peaks, as expected.

By using the method of moments by Van Vleck,[16] we provide a quantitative analysis of the shape and width of the NMR lines. We have calculated the moments for a 100% abundant ^{29}Si diamond lattice, including 1963 atoms for the calculation of the second moment, M_2, and 95 atoms for the fourth moment, M_4 (see first and second columns in Table I). The line shape is dependent on the value of $M_4/[3\times(M_2)^2]$. If this value is much larger than 1, the line shape is Lorentzian, if it is equal to 1, the line shape is Gaussian, and if it is significantly smaller than one, a double peak appears.[15] As can be derived from the data in Table I, the theoretical value of $M_4/[3\times(M_2)^2]$ is smaller than 1 for all crystal orientations. The smallest value is obtained for the [111] orientation, for which line splitting is observed.

The full width at half maximum (FWHM) of a resonance

TABLE I. The theoretical values of M_2 and M_4 in the case of dipolar interactions are given for the three main crystal orientations in the first and second columns. The third column shows the experimental values of M_2 derived from the data of Fig. 2 and the fourth and fifth columns give the fractional increase of M_4 if J-coupling is present. The data in the table are results of theoretical calculations, unless otherwise specified.

	M_2 (100 Hz)^2	M_{4_d} (100 Hz)^4	M_2 [a] (100 Hz)^2	M_{4_J}/M_{4_d} [b]	M_{4_J}/M_{4_d} [c]
[100]	5.86	66	16	0.550	0.043
[110]	36.9	2970	52	0.065	0.005
[111]	47.3	3880	63	0.063	0.005

[a]Experimental results.
[b]$J=180$ Hz.
[c]$J=50$ Hz.

line is directly proportional to M_2 and inversely proportional to M_4, which is illustrated by the following formula for, respectively, a Gaussian-shaped and Lorentzian-shaped resonance line (truncated Lorentzian):

$$\mathrm{FWHM}_{\mathrm{Gaus}}=2.36\sqrt{M_2}, \tag{4}$$

$$\mathrm{FWHM}_{\mathrm{Loren}}\approx 1.8M_2\sqrt{\frac{M_2{}^2}{M_4}}. \tag{5}$$

It is clear from Table I that the narrowest line is expected for the [100] orientation.

In the third column of Table I, we give the experimental values for the second moment M_2. Comparison with theoretical predictions demonstrates that the experimental FWHM is larger than expected. This is partially due to magnetic field inhomogeneities and susceptibility effects, which in our setup increase the width of the resonance line by approximately 100 Hz (see Sec. VI). This broadening increases M_2 and the increase is most pronounced for the narrowest line. It has also been mentioned in the previous section that there is a 10° error in the crystal orientation of the sample. Since the [100] orientation has the narrowest line, any deviation from this orientation will result in an increased linewidth. Both factors therefore affect most strongly the experimental data for the [100] orientation, which explains the differences between the first and third columns of Table I.

To obtain information on the J-coupling, we have calculated M_4 based on dipolar interactions only, M_{4_d}, and the additional M_4 if J-coupling is included, M_{4_J} (see fourth and fifth columns in Table I). Two representative values of the J-coupling have been used (see Sec. IV). The second moment M_2 is not changed by the presence of J-coupling, since it is an exchange-type interaction. The values in Table I show that the increase of M_4 is most pronounced for the [100] orientation, where an increase of M_4 with 55% is expected for a J-coupling of 180 Hz. As discussed before, increases in M_4 correspond to a narrowing of the resonance line. Therefore, in order to determine the J-coupling based on this model, it would be desirable to reduce the line broadening due to magnetic field inhomogeneity and uncertainty in sample orientation by the use of appropriate sample shapes and state-of-the-art equipment. In such conditions, we would expect a reduction of these unwanted broadening effects to less than about 5 Hz, and a more quantitative study of the J-coupling could be performed.

VI. EXPERIMENTAL RESULTS FOR NATURALLY ABUNDANT SILICON

In naturally abundant silicon, the ^{29}Si atoms are very dilute (4.7% ^{29}Si) and the overall effect of dipolar interactions on the NMR spectrum is small. Dipolar interactions are only significant for neighboring ^{29}Si atoms, in which case Eqs. (2) and (3), which are valid for isolated pairs of ^{29}Si atoms, are a good model for the experimental situation. All isolated ^{29}Si atoms precess with the unperturbed Larmor frequency. The NMR spectra for naturally abundant silicon are displayed in Fig. 3 for the three main crystal orientations. The spectra

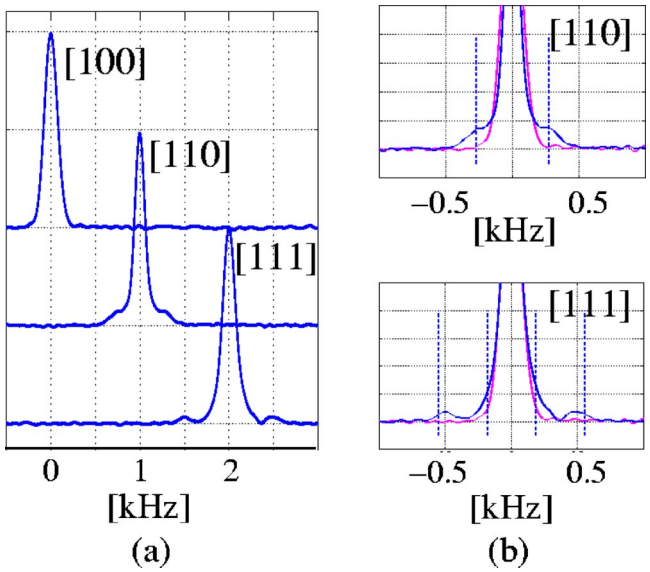

FIG. 3. (a) NMR spectra of naturally abundant silicon for three orientations: $B_0\|$ [100], $B_0 \|$ [110] (spectrum shifted by 1 kHz), and $B_0 \|$ [111] (spectrum shifted by 2 kHz). The spectra are averages over 7 to 17 experiments. The horizontal axis is offset by 59.5744 MHz; the vertical axis is arbitrary. (b) Comparison of the line shape for $B_0 \|$ [100] (dashed curve) with the line shape for $B_0 \|$ [110] (top figure) and $B_0 \|$ [111] (bottom figure). The dashed vertical lines indicate the position of the theoretically calculated resonance frequencies of the side peaks.

TABLE II. For a random distribution of 4.7% ^{29}Si atoms in a ^{28}Si matrix, the theoretical ratio of the area under the side peaks versus the area under the full spectrum has been calculated for the three main crystal orientations. In the [111] orientation, only the outer two side peaks are considered. The experimental value of the ratio is obtained from the data of Fig. 3.

	Theoretical	Experimental
[100]	0	0
[110]	0.19	0.22 ± 0.015
[111]	0.047	0.06 ± 0.015

have been normalized, such that the amplitude of the central resonance peak is the same for the three spectra.

For all crystal orientations, the central resonance line is very narrow (FWHM$=170$ Hz) and results from nearly isolated ^{29}Si nuclei. The width of this peak is mainly due to inhomogeneity of the magnetic field over the sample volume since spin-echo experiments have shown that the effective linewidth is less than 50 Hz. Some finer structure is visible for the [110] and [111] orientations. For better comparison, the [100] resonance line is plotted on top of, respectively, the [110] and [111] resonance lines in Fig. 3(b). The side peaks are produced by pairs of ^{29}Si nuclei and the frequency separation depends on the orientation of the axis of the pair with respect to the magnetic field. As expected from Eq. (2), the data for the [110] orientation shows the presence of a side structure with a splitting of about 550 Hz. In the spectra of the [111] orientation, a clear set of side peaks is visible with a splitting of about 1000 Hz [Eq. (3)] and an additional two peaks at roughly 367-Hz splitting. Small deviations of the line splittings from the theoretical predictions are due to inaccurate orientation of the sample with respect to the magnetic field. The side structure has been observed in previous experiments with silicon,[17] in which optical pumping has been used to overcome the low signal-to-noise ratio of the ^{29}Si NMR spectrum.

The amplitude of the side peaks is directly proportional to the number of nuclei that form pairs. If the ^{29}Si atoms are randomly distributed in the ^{28}Si matrix, a fraction of 0.047^2 of the atoms forms ^{29}Si pairs with a specific bond orientation. For the [111] orientation, for example, the outer two peaks are formed by a ^{29}Si pair whose pair axis is parallel to B_0. Every atom can be part of only one such pair (see Fig. 1). Therefore, assuming a random distribution of the ^{29}Si atoms, the area under the outer two side peaks should be 0.047 times the area under the full spectrum. In the [110] orientation, on the other hand, there are four possible pair configurations containing the same ^{29}Si nucleus and producing the same line splitting. Therefore, to first order, the area under the two side peaks is expected to be $0.047 \times 4 = 0.19$ times the area under the full spectrum. These theoretical predictions for a random distribution are summarized in Table II together with the experimental values obtained from the data in Fig. 3. Taking into account the difficulty in accurate positioning of the sample, we conclude that there is very good agreement between theory and experiment, and that the distribution of the ^{29}Si atoms resembles a random distribution.

From the previous discussion, it is clear that NMR can be used to check the distribution of ^{29}Si atoms in a ^{28}Si matrix. More precisely, the amount of pairs of ^{29}Si atoms versus single ^{29}Si atoms can be derived. The same technique can be used to verify the quality of future isotopically engineered structures, such as atomic planes of ^{29}Si atoms in a ^{28}Si matrix. In this case, no nearest-neighbor ^{29}Si pairs exist, which results in the absence of side peaks with 1100-Hz splitting if B_0 is oriented along one of the $\langle 111 \rangle$ directions of the crystal. If NMR becomes sensitive enough, it could also be used to check the overall uniformity of the distribution of substitutional dopants in bulk silicon, such as ^{31}P atoms, for example (nuclear spin $\frac{1}{2}$).

Finally, we have measured the uniform chemical shift F_{Si} of single-crystal silicon with respect to $(CH_3)_4Si$ (TMS). As mentioned in Sec. IV, there is negligible anisotropy of the chemical shift. The experiment has been performed with naturally abundant silicon and the substitution method has been used. A chemical shift of $F_{\mathrm{Si}} = (\nu_{\mathrm{Si}} - \nu_{\mathrm{TMS}})/\nu_{\mathrm{TMS}} = -82.5 \pm 1$ ppm is obtained.

VII. CONCLUSION

In conclusion, we have presented NMR spectra of ^{29}Si-enriched and naturally abundant single-crystal silicon. The spectra show significantly different line shapes if the B_0 field is parallel with, respectively, the [100], [110], or [111] directions and we show that this is due to the anisotropy of the magnetic dipole-dipole interaction. For the ^{29}Si-enriched sample, we analyze the effect of the scalar coupling on the line shape and describe how a more quantitative value can be obtained with state-of-the-art equipment. Furthermore, we have proposed NMR spectroscopy as a tool to characterize the randomness of the distribution of dilute substitutional magnetic nuclei in single-crystal samples with a diamond structure. This technique is based on the ratios of areas of NMR resonance peaks.

ACKNOWLEDGMENTS

The authors would like to acknowledge Mark Sherwood for very useful discussions and Kai-Mei Fu and Thaddeus Ladd for help with the manuscript. We are also grateful to the IBM Almaden Research Center, San Jose, for supporting us with NMR spectroscopy equipment. This work was supported by DARPA under the QuIST initiative.

*Email address: verhulst@leland.stanford.edu
†Also at Sektion Physik, Ludwig-Maximilians-Universität, D-80797 München, Germany.
‡Also at NTT Basic Research Laboratories, 3-1 Morinosato-Wakamiya, Atsugi-shi, Kanagawa 243-01, Japan.

[1] B.E. Kane, Nature (London) **393**, 133 (1998).
[2] T.D. Ladd, J.R. Goldman, F. Yamaguchi, Y. Yamamoto, E. Abe, and K.M. Itoh, Phys. Rev. Lett. **89**, 017901 (2002).
[3] K.-I. Takyu, K.M. Itoh, K. Oka, N. Saito, and V.I. Ozhogin, Jpn. J. Appl. Phys., Part 2 **38**, L1493 (1999).

[4] Wafers available through Isonics, 5906 McIntyre Street, Golden, CO 80403.
[5] G. Lampel, Phys. Rev. Lett. **20**, 491 (1968).
[6] N.T. Bagraev, L.S. Vlasenko, and R.A. Zhitnikov, Pisma Zh. Éksp. Teor. Fiz. **23**, 639 (1976) [JETP Lett. **23**, 586 (1976)].
[7] A. Abragam, *Principles of Nuclear Magnetism* (Oxford University, New York, 1999), p. 391.
[8] H. Holloway, K.C. Hass, M.A. Tamor, T.R. Anthony, and W.F. Banholzer, Phys. Rev. B **44**, 7123 (1991).
[9] M.H. Sherwood, in *Encyclopedia of NMR*, edited by D.M. Grant and R.K. Harris (Wiley, New York, 1996), Vol. 2, p. 1322.
[10] M.A. Ruderman and C. Kittel, Phys. Rev. **96**, 99 (1954).
[11] W. Meyer, J. Chem. Phys. **51**, 5149 (1969).
[12] H.C. Marsmann, in *Encyclopedia of Spectroscopy & Spectrometry*, edited by J.C. Lindon, G.E. Tranter, and J.L. Holmes (Academic, California, 2000), Vol. 3, p. 2031.
[13] G.E. Pake, J. Chem. Phys. **16**, 327 (1948).
[14] K. Lefmann, B. Buras, E.J. Pedersen, E.S. Shabanova, P.A. Thorsen, and F.B. Rasmussen, Phys. Rev. B **50**, 15 623 (1994).
[15] A. Abragam, *Principles of Nuclear Magnetism* (Oxford University, New York, 1999), p. 103.
[16] J.H. Van Vleck, Phys. Rev. **74**, 1168 (1948).
[17] L.S. Vlasenko, Pisma Zh. Tekh. Fiz. **10**, 1102 (1984) [Sov. Tech. Phys. Lett. **10**, 467 (1984)].